Cr-doped porous silica glass as a model material to describe Phillips catalyst properties

UNIVERSITÀ DEGLI STUDI DI TORINO

A. Budnyk, A. Damin, C. Barzan, E. Groppo, C. Lamberti, S. Bordiga, A. Zecchina, "Cr-doped porous silica glass as a model material to describe Phillips catalyst properties", *J. Catal*., **308** (2013) 319-327.

DOI: 10.1016/j.jcat.2013.08.016

http://www.sciencedirect.com/science/article/pii/S0021951713003060

Cr-doped porous silica glass as a model material to describe Phillips catalyst properties

Andriy Budnyk, Alessandro Damin, Caterina Barzan, Elena Groppo, Carlo Lamberti, Silvia Bordiga* and Adriano Zecchina

Department of Chemistry, NIS Centre of Excellence, University of Turin, Via G. Quarello 15 A, I-10135 Torino, Italy

Graphical abstract

Cr-doped mesoporous silica glass offers the possibility to follow spectroscopically the structure and reactivities of highly diluted Cr species in Phillips-type catalyst.

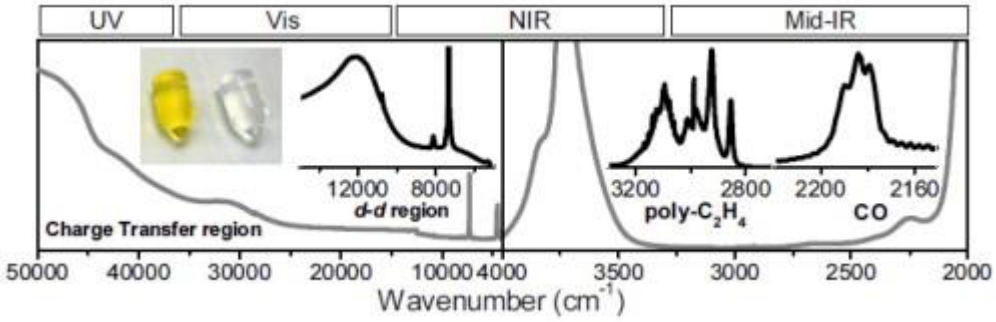

Abstract

Cr-doped mesoporous silica glasses with Cr loading in the 0.01–0.5 wt% range were synthesized by one-pot acid catalyzed sol–gel route in form of monoliths. The absence of light scattering in the whole IR and UV–Vis–NIR region makes them ideal systems to investigate the optical and structural properties of grafted Cr sites by means of transmission spectroscopy, even in the highest diluted case, on which this contribution is mainly focused. For these reasons, Cr-doped porous silica monoliths are proposed here as models for the well-known Phillips catalyst for ethylene polymerization. It is demonstrated that, even when chromium is extremely diluted (0.01 wt%), the electronic and structural properties of the Cr sites (both in the oxidized and reduced forms) are very similar to those of Cr sites on standard, aerosil-based, Phillips catalysts (with a Cr content of 0.5 and 1 wt%): a distribution of Cr sites differing in the coordination ability is always present, irrespective of the Cr concentration and of the silica support. Nevertheless, the possibility to perform UV–Vis spectroscopy in transmission allowed to add unprecedented information on the relative intensity of bands due to charge transfer and d–d transitions. In situ ethylene polymerization was followed by means of both IR and UV–Vis spectroscopy in transmission on the sample having the lowest Cr loading (0.01 wt%), showing that the precursor species can be easily traced from the first steps of polymerization and that they are very similar to those observed on more concentrated catalysts.

1. Introduction

Herein, we present the synthesis, characterization, and catalytic properties of one-pot Cr/silica monoliths characterized by very low chromium concentration (0.01 wt%), as models for very diluted Phillips catalyst for ethylene polymerization [1]. To fully justify the reasons behind the choice of a silica monolith as a support of Cr(VI) and Cr(II) species, it is necessary to review (i) the state of knowledge concerning the parent Cr(VI)/SiO_2 and Cr(II)/SiO_2 catalysts (with specific attention to the open problems related to the structure of the chromium sites, their spectroscopic properties, and the ethylene polymerization mechanism) and (ii) the most appealing properties of silica monoliths.

Discovered in 1951 [2] and progressively modified and evolved, nowadays, the Phillips catalyst is a highly versatile system accounting for the production of several types of high density (HDPE) and linear low density (LLDPE) polyethylenes, making it one of the world's most important industrial catalysts for over half a century [3]. For this reason, it has been and still is the subject of an intense industrial and academic research, both from an experimental [1], [3], [4], [5], [6], [7], [8], [9], [10], [11], [12], [13], [14], [15], [16], [17] and [18] and from the theoretical point of view [19], [20], [21], [22] and [23]. The industrial importance of this catalyst only partially justifies the persisting scientific interest on it; in fact, the peculiar properties of its active sites make it a perfect playground for basic spectroscopic investigations applied to catalysis [4], [6] and [7].

The polymerization of ethylene efficiently occurs in mild conditions on both Cr(VI) and Cr(II) sites grafted on silica. In a typical catalyst containing 0.5 wt% of chromium, the grafted sites are *isolated* [6]. This implies that the initiation step of ethylene polymerization occurs on isolated sites. However, it is not yet clear whether the participation of more than one site could play a significant role during the propagation or termination steps [13]. In this regard, pioneering works by Hogan et al. [24] suggested that the intrinsic catalytic activity per chromium site increases upon decreasing the chromium loading, reaching a maximum for a 0.01 wt% of Cr. These data have encouraged the preparation and study of very diluted samples, which is one of the reasons at the basis of the present investigation.

Silica-grafted Cr(VI) and Cr(II) sites can be converted one into the other upon reduction and oxidation cycles [6]. When the red-ox treatment is carefully conducted on sufficiently low concentrated samples (Cr loading below 0.5 wt%), the obtained chromium sites are characterized by a single oxidation state, explaining why diluted catalysts were chosen as model systems for spectroscopic studies throughout the years [4], [6], [7], [25], [26] and [27]. However, although uniform from the point of view of the oxidation state, a distribution of different types of chromium sites, characterized by slight variations in structure, is usually identified and reflects the amorphous nature of the silica support. Heterogeneity is more pronounced for the Cr(II)/SiO_2 catalyst (with respect to the oxidized form), for which it has been demonstrated that a variable number of weak siloxane ligands can enter into the coordination sphere of the grafted Cr(II) sites [6], influencing their coordination ability. The structural heterogeneity of chromium sites is usually considered as responsible for the broad molecular weight

distribution characterizing the Phillips HDPE [1] and [12]. Numerous studies demonstrated that the use of probe molecules is a powerful method for the characterization of different chromium sites [6], [28] and [29]. For example, Cr(II) sites display an outstanding capacity to form a variety of polycarbonyl, polynitrosyl, and mixed carbonyl–nitrosyl coordination complexes depending on the different chemical environment surrounding the metal site [25], [27], [28], [29], [30], [31] and [32]. One of the main problems that will be faced in the present investigation is whether the distribution of different chromium sites can be modified by changing the support or acting on the chromium concentration.

From the brief summary discussed above, the interest in the preparation and characterization of model Cr/SiO_2 catalysts with a very low chromium loading and a different silica support clearly emerges. We turned our attention toward porous silica monoliths because, following common sol–gel methods, it is possible to obtain monoliths displaying a high surface area (higher than 500 $m^2\ g^{-1}$) and characterized by the absence of any significant light scattering in the whole UV–Vis–NIR and Mid-IR regions. Both properties are expected to facilitate the spectroscopic investigation of the structure and the catalytic activity of very diluted metal centers, because they allow to obtain solution-like spectra by simply applying transmittance-based spectroscopic methods. In particular, thick samples can be studied (in contrast to diffusely scattering powders), thus greatly increasing the spectroscopic sensitivity and avoiding artifacts and distortions associated with the diffuse reflectance methods (*vide infra*).

A few examples of the advantages of using silica monoliths as supports for transition metal ions are present in literature. Of particular interest in this context, are the works of Stiegman et al., who prepared and characterized by Raman, NMR and EXAFS spectroscopies $V(V)/SiO_2$ [33] and [34] and $Cr(VI)/SiO_2$ [14] xerogels at different metal concentrations. We developed a similar one-pot synthesis method (following the sol–gel synthesis protocol of Weiping and Lide [35]), which guarantees a homogeneous distribution of the metal species in the glass and a good control of the metal loading. The use of monoliths as model supports presents two main advantages. (i) In the UV–Vis–NIR region, it is possible to determine the solution-like spectrum of grafted Cr species. This fact allows to estimate with unprecedented accuracy the real intensity ratio between d–d and charge transfer (CT) bands and to compare the obtained results with those of homogeneous complexes having similar structure and valence state. (ii) The total absence of scattering allows to increase the thickness of the monoliths during transmission FT-IR experiments, thus allowing to investigate very diluted samples (Cr concentration in the 0.1–0.01 wt% range), reaching Cr loadings not accessible on standard powdered materials. These advantages play a fundamental role in understanding the role of silica support and Cr concentration in determining the structure and the potential sites cooperation in the polymerization mechanism.

2. Materials and Methods

2.1. Synthesis

2.1.1. Monolith synthesis.

Tetraethyl orthosilicate (TEOS) was added to a mixture of anhydrous ethanol and

distilled water in molar ratio of 1:4:20, respectively, under stirring at room temperature. The pH was adjusted to about ~1–2 by drop-wise addition of diluted (1:10 vol.) nitric acid, and the mixture was left to stir for 1 h. TEOS (98%, Aldrich), nitric acid (69.0%, Aldrich), and ethanol (puriss. p.a., Fluka Analytical) were used as received; pure water (9 MΩ cm at 25 °C) was obtained by a Millipore Direct Q system.
In order to obtain a Cr-doped gel, a proper solution of CrO_3 in water was added to get the desired chromium loading with respect to SiO_2 content. Most of the data showed in this paper refer to 0.01 wt% loading, but samples having Cr concentration in the 0.05–0.5 wt% range were also prepared. The different mixtures were poured into plastic tubes and sealed. Tubes were kept in a pre-heated oven at 323 K for 2–3 days until occurrence of gelation. Then temperature was set at 353 K for a week of aging. For the drying step, the tubes were pin-holed to allow a slow evaporation of the solvent, and the temperature was gradually rised over a week up to 393 K. The dry xerogels were slowly heated in air at 873 K in 15 h and calcined at the same temperature for 1 h.

2.1.2 Synthesis of the standard Phillips catalyst.

Reference Cr/aerosil samples were prepared by impregnating a SiO_2-aerosil (surface area ca. 350 $m^2\ g^{-1}$) with an aqueous solution of CrO_3 to give a Cr/SiO_2 ratio of 1.0 and 0.5 wt%, following the recipe reported elsewhere [6]; the former was used for IR measurements and the latter for UV–Vis spectroscopy.

2.2. Macroscopic properties and samples nomenclature

Both fumed silica (aerosil) and gel-derived silica (porous glass) are amorphous solids of SiO_2 chemical composition; however, they are characterized by a different particle aggregation. Aerosil consists of non-porous particles of nanometric size, while sol–gel forms an open framework with multiple mesopores. A different structure affects the macroscopic properties and the appearance of the two silica types: aerosil is a fluffy white powder, whereas glass monoliths are transparent.
Fig. 1 shows the outlook of silica monoliths with chromium content ranging from 0.5 to 0.01 wt%, compared to pure silica monolith. All monoliths are transparent and exhibit a homogeneous color across monolith's volume, witnessing a uniform dispersion of chromium species. The comparative study of whole set of monoliths will be reported in an incoming paper. Hereafter, we will focus our attention on the most diluted case (0.01 wt%).
The samples will be labeled with both chromium content (wt%) and type of silica support – M (monolith) or P (powder). Thus, Cr0.01M and Cr0.1M indicate monoliths containing 0.01 and 0.1 wt% of Cr, respectively, whereas Cr0.5P and Cr1.0P stay for Phillips catalyst obtained from aerosil powder.

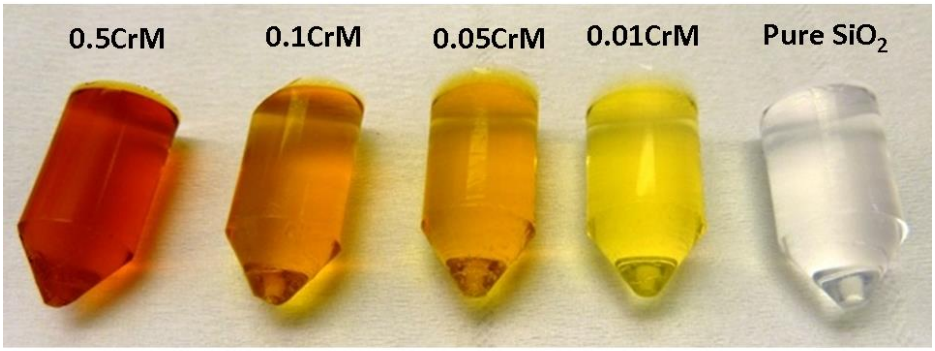

Fig. 1. Cr-doped monoliths after calcination at 873 K with chromium loading (from left to right) of: 0.5, 0.1, 0.05, 0.01 wt% and pure SiO_2.

2.3. Activation procedure

Cr-doped monoliths (cut in order to obtain slices of optimized thickness) and Cr/aerosil samples (in the form of self-standing pellets) were activated directly inside the measurement cells (for IR or UV–Vis) following the same procedure, as reported elsewhere. Briefly, the samples were outgassed at 923 K for 1 h and successively oxidized at 923 K by two subsequent doses of O_2 (100 mbar) alternated by an outgassing step to remove the reaction products. It was previously demonstrated that this treatment provides only Cr(VI) sites [6]. Reduction of Cr(VI) to Cr(II) was obtained by a successive reductive treatment at 623 K in CO (two subsequent doses of 100 mbar alternated by an outgassing step), followed by CO removal at the same temperature; finally, the samples were cooled down to room temperature.

2.4. Characterization techniques

Textural and structural properties of monoliths were investigated by N_2 adsorption measurements and X-Ray Powder Diffraction (XRPD), respectively. In both cases, pieces of monoliths were ground into powder. The surface area and the pore size distribution (PSD) were obtained using a multiple point nitrogen gas adsorption analyzer ASAP 2020 by Micromeritics. Prior to N_2 sorption, the portion of the sample of ~0.1 g weight was outgassed and heated in vacuum pressure lower than 1 Pa at 423 K for 2 hours. The specific surface area was estimated in relation to the mass of the outgassed sample. Specific surface area was calculated by BET method [Brunauer, 1938 #1087] and the PSD was calculated on the basis of BJH method [Barrett, 1951 #1088]. The XRPD pattern was collected by a Philips X'Pert PRO Diffractometer with a grafite-monochromated Cu Kα (λ = 1.54 Å) radiation operating at 45 kV and 40 mA. SEM images have been obtained by SEM EVO 50XVP Carl Zeiss AG, equipped with an EDS instrument for compositional analysis.

Optical and vibrational properties of all the samples were investigated by combining transmittance and reflectance approaches in the UV-Vis-NIR regions depending on the morphology of the samples (monolith or powder). When possible, for all absorption spectroscopies, the transmission mode geometry should be adopted as it guarantees to optimize the experimental spectra in terms of signal/noise ratio; the best conditions are

reached when in the Lambert-Beer equation ($I_1 = I_0\, e^{-\mu x}$), μx lies in the 0.5-2.0 range. For very diluted samples (very low μ), the thickness x should be increases to keep the μx product within the optimal interval. However, this is possible only when light absorption is the major cause of the attenuation of the primary beam, thus cannot be applied in the UV-Vis region for powdered materials. High surface area SiO_2 powders, such as aerosil, are characterized by very small average particle dimension D (D ~ 20 nm) that makes the ratio $D/\lambda << 1$ in the whole UV–Mid-IR region of the electromagnetic spectrum. Under such circumstances light scattering is described by the Rayleigh scattering, that exhibits a λ^{-4} dependence [Schumann, 2012 #1089] and is much more efficient than photon absorption. This is the reason why the diffuse reflectance (DR) mode is used for that class of materials in the UV-Vis region (short λ). On the contrary, the λ^{-4} dependence is much less penalizing in the Mid-IR region; therefore, transmission FT-IR spectroscopy is usually employed to investigate the Cr-aerosil catalyst in form of very thin self-supported wafers [Groppo, 2005 #329; Lamberti, 2010 #484; Groppo, 2013 #1067]. Herein, we exploited the absence of scattering and the optical homogeneity of our monoliths to perform Mid-IR and UV-Vis-NIR spectroscopic measurements in transmission mode on samples of optimized thickness x (different for the Mid-IR, NIR and UV-Vis regions).

A Varian Cary5000 spectrophotometer was employed for both transmittance and reflectance UV-Vis-NIR measurements. For Cr/monoliths, a regular piece of proper thickness was measured in a 10 mm UV-cell that can be connected to a vacuum line allowing activations and gas dosages. Data were collected in transmission at a 2 nm resolution, and successively converted in absorbance. UV-Vis spectra of Cr/aerosil were collected on samples in the form of thick pellets inserted in a cell that allows in situ activation and gas dosages. The measurements were performed in Diffuse Reflectance mode (%R) at 2 nm resolution and successively converted into Kubelka-Munk (K.M.) values.

Infrared spectra were recorded on a Bruker Vertex 70 instrument, at 2 cm^{-1} resolution. Cr/monoliths and Cr/aerosil samples were measured in the form of a regular piece of proper thickness and of self-standing pellet, respectively, inside a cell allowing activations and gas dosages.

3. Results and Discussion

3.1. Basic characterization of the pure monolith

3.1.1. Structural and textural properties of the pure monolith

The structural and textural properties of the pure silica monolith are summarized in Fig. 2. The XRPD pattern (Fig. 2a) is typical of an amorphous material, being characterized by an ill-defined peak centered around $2\theta = 22°$ ($d \sim 4.0$ Å) and by broad higher order structures around $2\theta = 45$ and 65° ($d \sim 2.0$ and 1.4 Å). Nitrogen adsorption–desorption measurements performed at 77 K (Fig. 2b) resulted into a Type IV isotherm according to IUPAC nomenclature [39] and [40], which is indicative of a mesoporous material. The resulting pore distribution is centered at about 4 nm (Fig. 2c). The desorption branch of the isotherm shows an hysteresis loop of Type H2 [41], which indicates capillary condensation in mesopores having a combined (cylindrical and spherical)

geometry. Turnover point of desorption branch at $p/p_0 \sim 0.4$ might be the evidence of cavitation prevailing over percolation effect. The calculated BET SSA value is 590 m^2/g.

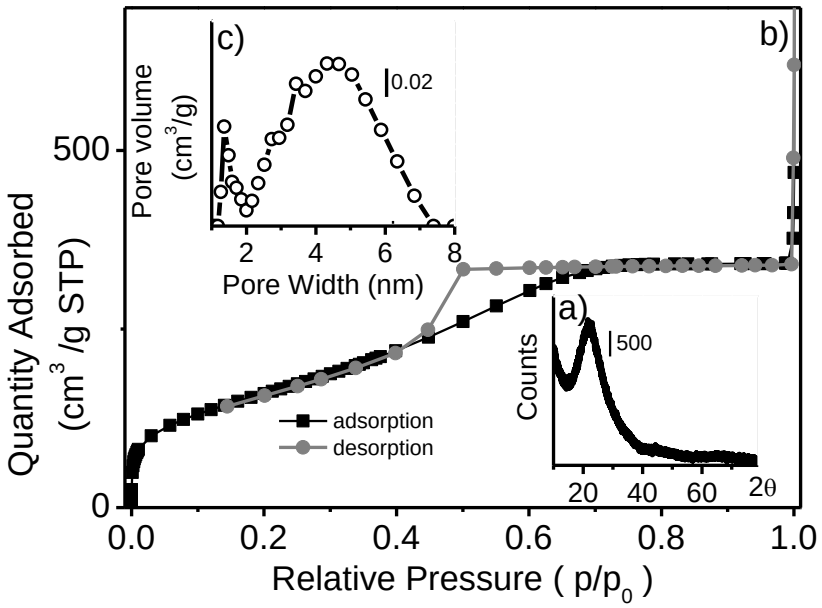

Fig. 2. Basic characterization of the pure silica monolith. Part (a): XRPD pattern (λ = 1.54 Å). Part (b): N_2 adsorption–desorption isotherms (77 K). Part (c) corresponding BJH width pore distribution.

3.1.2. Surface hydroxylation of the pure monolith in comparison with aerosil

Treatment at elevated temperatures in dynamic vacuum leads to progressive dehydroxylation of the silica surface. According to the Zhuravlev model [42], treatment at 923 K reduces the hydroxyl population at the level of 1–2 OH/nm^2. FT-IR spectroscopy was widely employed in the characterization of the surface hydroxylation of silica-based materials [42], and the similarity between the FT-IR spectra of silica gel and aerosil was previously highlighted [43], [44] and [45].

Fig. 3 reports the FT-IR spectrum of a thick slice ($x \sim 1$ mm) of the pure silica monolith activated at 923 K in the extended 7500–900 cm^{-1} range. Both fundamental O–H stretching (4000–3500 cm^{-1} range) and silica framework stretching modes below 2000 cm^{-1} are out of scale. For sake of comparison, the spectrum of a thin aerosil pellet activated at the same temperature is reported in the 6000–900 cm^{-1} range (inset). The advantage in using the monolith over aerosil is evident: despite the greater thickness, the spectrum of the monolith shows a flat profile in the whole region, whereas the spectrum of aerosil is characterized by a scattering profile which increases upon increasing ν (decreasing λ).

The possibility to work with thick slices of silica monoliths without encountering scattering problems allows to detect very weak spectroscopic features that escape detection when thin pellets of conventional aerosil are used. For example, the strong and narrow absorption band at 7330 cm^{-1} is assigned to the first overtone of the stretching vibration of isolated silanols groups absorbing at 3750 cm^{-1}; the band centered at 4527 cm^{-1} is assigned to the combination of OH stretching with the SiOH bending mode [46]; whereas bands at 2650 and 2246 cm^{-1} are weak combination of the

framework modes. These IR absorption bands are not visible in the IR spectrum of standard aerosil.

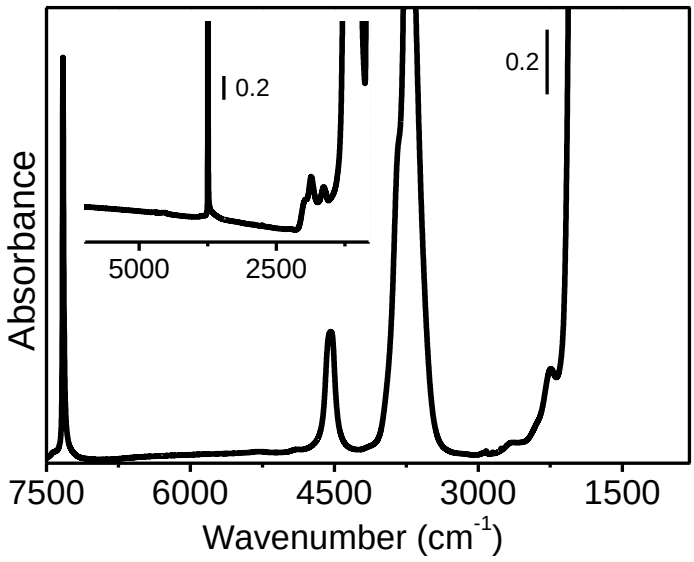

Fig. 3. Mid-IR spectra of pure silica monolith and of aerosil pressed powder (inset) after thermal activation at 923 K for 1 hour (see details in the text).

The experiment reported in Fig. 3 clearly shows that by continuous increase in the silica monolith thickness *x*, it is possible to detect IR absorption bands associated with vibrational modes characterized by progressively lower extinction coefficients. As far as the Cr-doped samples are concerned, the possibility to increase the monolith thickness *x* up to 10–20 times that of Cr/aerosil pellets allowed us to investigate very diluted samples, whose spectroscopic properties would not be measurable on conventional aerosil-based materials. We will show that this approach is even more useful in the UV–Vis–NIR region.

3.2. Optical spectra of oxidized and reduced Cr/SiO_2: comparison between monolith and aerosil supports

For homogeneous complexes in solution, electronic transitions having a CT character are usually very intense and are characterized by a molar extinction coefficient in the 10^3–10^4 range. These transitions are consequently at least 1 or 2 order of magnitude more intense than transitions having a d–d character [47]. For samples where surface scattering is negligible (i.e. liquids or monoliths), the concentration of the analyte and the sample thickness can be tuned continuously in order to optimize the spectroscopic datum. On the contrary, for samples where surface scattering is relevant, the diffuse reflectance mode is required and less degrees of freedom are available. In particular, (i) sample's thickness cannot be tuned, because it must be large enough to be considered as infinite; (ii) an homogeneous analyte dilution is much more difficult to be achieved on a solid surface than in a liquid; and (iii) band intensities are affected by the severe λ dependence of the Rayleigh scattering and by the fact that scattering is enhanced for wavelengths comparable with particles dimensions; this causes a change in the intensity ratio between bands appearing in different spectral ranges.

An example of the last concept is illustrated in Fig. 4, where the UV–Vis–NIR data of Cr-doped silica monoliths (in both oxidized and reduced forms) collected in transmission mode (parts a and c) are compared to those of the corresponding powdered Cr/aerosil collected in reflectance mode (parts b and d). The DR spectra of powdered Cr(VI)/SiO_2 samples were largely discussed in the specialized literature as a function of Cr loading [4], [6], [7], [48] and [49]. According to the literature, the three intense bands observed in the spectrum of Cr0.5P (part b) at ca. 42,000 cm^{-1}, 32,000 cm^{-1}, and 22,000 cm^{-1} are assigned to CT bands of grafted monochromate species. The same bands are observed in the UV–Vis spectrum of the much more diluted Cr0.01M sample (part a, collected in transmission mode), although characterized by a different relative intensity. The correct intensity ratio obtained from the transmission experiment is $I_{22,000}$:$I_{32,000}$:$I_{42,000}$ ~ 1:6:24, whereas in the spectra collected in DR mode $I_{22,000}$:$I_{32,000}$:$I_{42,000}$ ~ 1:1.5:1.5. Comparison of the UV–Vis–NIR spectra shown in Fig. 4 a and b demonstrates that the intensity of CT bands in DR spectra is heavily distorted.

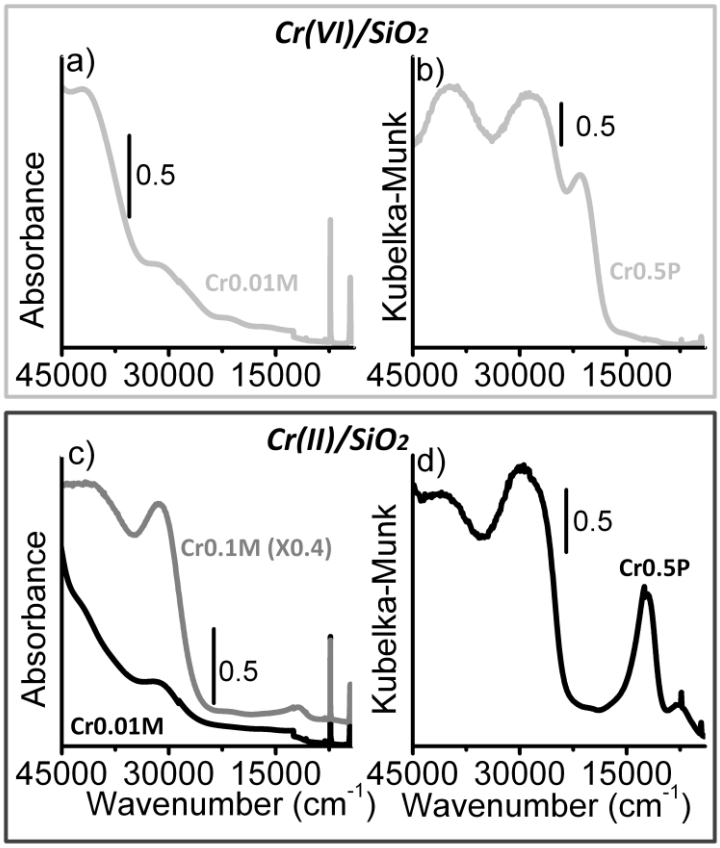

Fig. 4. UV-Vis-NIR spectra collected in transmittance mode on Cr0.01M sample in its oxidized (part a) and reduced (part c) forms, compared to the UV-Vis-NIR spectra collected in reflectance mode on Cr0.5P sample in its oxidized (part b) and reduced (part d) forms. In part c) also the spectrum of the reduced Cr0.1M sample is shown, vertically translated for clarity and multiplied by 0.4, to better show the d-d transition of Cr(II). Note that in the spectra collected in transmittance mode (parts a and c) the narrow bands at 7335 and 4539 cm^{-1} are due to overtones of the vibrational modes of surface hydroxyl groups.

Reduction of Cr(VI)/SiO_2 samples in CO at 623 K leads to the formation of Cr(II)/SiO_2 and to a change in color from yellow to light blue. The DR UV–Vis–NIR spectrum of Cr(II)/aerosil is well known in the literature and characterized by two intense band centered around 42,000 and 30,000 cm^{-1} (having a CT character) and by two d–d bands at 12,000 and 7500 cm^{-1} of d–d character. An example is shown in Fig. 4d for Cr0.5P. These bands are usually considered as the finger-prints of well isolated Cr(II) sites. However, as for the oxidized case, the intensity ratio of the CT bands is misleading. On the contrary, the UV–Vis–NIR spectra of Cr(II)/monoliths collected in transmission mode (Fig. 4c) allow to appreciate, for the first time, the true relative intensity ratio between CT and d–d bands. When the two CT bands are in scale (Cr0.01M sample), the two d–d bands are scarcely visible, as expected on the basis of their much smaller extinction coefficient (about one order of magnitude weaker than for the CT transitions) [47]. On the contrary, when the Cr loading is increased by one order of magnitude (Cr0.1M sample), the d–d bands are well visible, but only the CT band at 30,000 cm^{-1} remains in scale. Comparison of the two UV–Vis–NIR spectra of Cr0.01M and Cr0.1M allows to establish the relative intensities of all the bands: I_{7500}:$I_{12,000}$:$I_{30,000}$:$I_{42,000}$ = 1:6:20:60.

The determination of the extinction coefficients for all the electronic transitions characterizing Cr(II) and Cr(VI) sites grafted on silica is a unique result of the use of silica monoliths as supports. These data constitute a valuable database that becomes available as reference for computer modeling studies aimed to describe electronic transitions.

3.3. CO adsorption at room temperature on reduced Cr(II)/SiO_2: a comparison between monolith and aerosil supports

3.3.1. IR spectroscopy

The UV–Vis spectra discussed in the previous section demonstrate that the electronic properties of grafted Cr(VI) and Cr(II) remain the same, irrespective of the type of silica support (mesoporous glass or aerosil powder) and of the chromium concentration. Nonetheless, the intrinsic broad character of the electronic transitions does not allow to finely characterize the local environment of the chromium sites. To achieve this aim, FT-IR spectroscopy of adsorbed CO as a probe molecule is one of the most employed method for characterizing Cr(II)/SiO_2 samples since many decades [6], [25], [29] and [50].

It is widely accepted that on Cr(II)/aerosil samples, CO reveals the presence of two types of Cr(II) sites, characterized by a different coordination ability: mono-carbonyl adducts are formed on the so called Cr_B(II) sites, whereas di-carbonyls are formed on Cr_A(II) sites [6], [25], [29] and [50], although slightly different interpretations can be found in the literature [51] and [52]. An example is shown in Fig. 5b that reports the FT-IR spectra of CO adsorbed at room temperature on Cr1.0P as a function of the CO equilibrium pressure. At high CO coverage (bold black spectrum), a characteristic triplet of absorption bands is observed, located at higher wavenumbers with respect to stretching of CO gas (dotted vertical line). The absorption band at 2190 cm^{-1} is assigned

to mono-carbonyls formed on $Cr_B(II)$ sites, whereas the two bands at 2184 cm^{-1} and 2179 cm^{-1} are assigned to the symmetric and asymmetric stretching of di-carbonyl adducts formed on $Cr_A(II)$ sites. Upon gradually reducing the pressure, the triplet transforms into a doublet of bands at 2190 and 2180 cm^{-1} (bold gray spectrum), the latter due to mono-carbonyls on $Cr_A(II)$ sites.

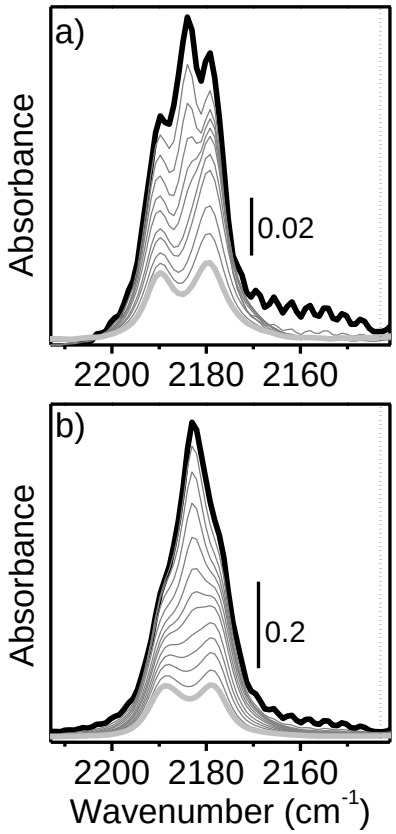

Fig. 5. Evolution of the FT-IR spectra of CO adsorbed at room temperature on Cr0.01M (part a) and Cr1.0P (part b) as a function of the CO equilibrium pressure (P_{CO}). Bold black spectra refer to the maximum CO coverage (P_{CO} =100 mbar); bold grey spectra are collected after prolonged outgassing at room temperature (irreversible CO species). Vertical dotted lines show the stretching frequency of CO in the gas phase.

When CO is dosed (100 mbar) at room temperature on Cr0.01M (Fig. 5a), a triplet of IR absorption bands very similar to those discussed for Cr0.5P is observed. Such similarity leads to the conclusion that the two samples are characterized by the same heterogeneity of Cr(II) sites, despite the difference of 2 orders of magnitude in the chromium loading. This observation suggests that the distribution of different chromium sites is not modified by acting on the chromium concentration. Going in more detail, small differences are observed in the FT-IR spectra of CO adsorbed on Cr0.01M and Cr0.5P. In particular, (i) the IR absorption bands of the triplet are narrower on the former, suggesting that inside each family, $Cr_A(II)$ or $Cr_B(II)$, the Cr(II) sites are more homogeneous on the monolith than on dispersed silica; (ii) the relative concentration of the two types of chromium sites is different, as evidenced by the integrated area of the IR absorption bands of adsorbed CO: $Cr_A(II)$ are relatively more

abundant than Cr_B(II) sites in Cr0.01M than in Cr1.0P; (iii) at high CO coverage, the relative intensity of the two IR absorption bands assigned to the asymmetric and symmetric ν(CO) modes of di-carbonyls formed on Cr_A(II) sites is different for the two samples, suggesting that the angle defined by the two CO ligands is also different. Whether these differences are due to the support or to the chromium dilution is difficult to infer.

As a conclusive remark concerning the spectra of adsorbed CO, it is important to stress that the use of monoliths allows to collect the FT-IR spectra of adsorbed CO on extremely diluted Cr(II)/SiO_2 samples, which is not possible for aerosil-supported samples.

3.3.2. UV-Vis spectroscopy

DR UV–Vis–NIR spectroscopy has been used in the past to complement the FT-IR results of CO adsorbed at room temperature on Cr(II)/SiO_2 samples. It is known that the d–d transitions characteristic of grafted Cr(II) sites are perturbed by CO adsorption, as a consequence of the increased ligand field around the Cr(II) sites [6] and [7]. A typical experiment is shown in Fig. 6b for Cr0.5P. Upon CO dosage, the d–d bands at 12,000 and 7500 cm^{-1} characteristic of coordinatively unsaturated Cr(II) sites, shift upward to 14,000 cm^{-1} and 8600 cm^{-1}, respectively, as a consequence of the formation of mono-carbonyl adducts on both Cr_A(II) and Cr_B(II) sites (bold light gray spectrum). Further increase in the CO equilibrium pressure (bold black spectrum) leads to the disappearance of the 14,000–8600 cm^{-1} doublet and to the growth of a new band at 20,000 cm^{-1}, which is assigned to di-carbonyls formation. The presence of an isosbestic point at 16,000 cm^{-1} confirms that mono-carbonyls are converted into di-carbonyl species.

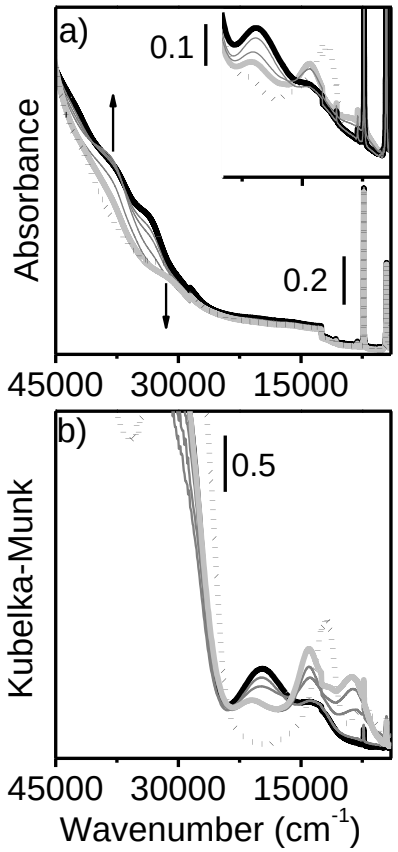

Fig. 6. Evolution of the UV-Vis-NIR spectra of CO adsorbed at room temperature on Cr0.01M (part a), Cr0.1M (inset in part a) and Cr1.0P (part b), as a function of the CO equilibrium pressure (P_{CO}). The spectra were collected in transmittance and reflectance mode for Cr-monoliths and Cr-aerosil, respectively. Dotted spectra: Cr(II)/SiO_2 samples before CO dosage; bold black spectra: maximum CO coverage (P_{CO} =100 mbar); bold light grey spectra: prolonged outgassing at room temperature (irreversible CO species).

3.4 Ethylene polymerization at room temperature on reduced Cr(II)/SiO_2 samples: a comparison between monolith and aerosil supports

The Phillips catalyst, both in the oxidized and reduced forms, is known for its ability to polymerize ethylene without the assistance of any activator [1]. In the first case, ethylene itself works as a reducing agent to bring chromium in a lower oxidation state. Reduction occurs during an induction time in which Cr(VI) is slowly reduced to Cr(II). At room temperature and low pressure, only a fraction of the Cr(II) sites (close to 10%) is able to initiate the polymerization reaction [53] and [54], although this fraction can be increased by raising the reaction pressure and temperature; it is supposed that the sites active at room temperature are those characterized by the highest coordinative unsaturation [55]. The remaining Cr(II) sites behave like spectators, and only molecules with strong d–π interaction ability (such as CO) are able to pull them from their more shielded position on silica surface, to form protruding surface carbonyl adducts [10]. It has been established that the initiation of ethylene polymerization on Cr(II)/SiO_2 occurs via a metallacycle mechanism [56]; less is known on the initiation on Cr(VI)/SiO_2[23] and [57]. Concerning the propagation and termination steps, the

participation of further Cr(II) sites in interaction with the formed polymer chains has not been excluded [13]. However, this effect should progressively loose importance by decreasing the Cr(II) concentration. In this perspective, a study of ethylene polymerization reaction on highly diluted Cr(II)/SiO_2 samples is of particular interest. Ethylene polymerization at room temperature on Cr0.01M was followed by time-resolved FT-IR spectroscopy, as shown in Fig. 7a. Immediately after contact with ethylene, intense IR absorption bands are clearly observed in the 3300–2800 cm^{-1} range, due to the asymmetric and symmetric ν(CH) vibrations of ethylene gas. Because of diffusion reasons, these absorption bands reach their maximum intensity only after a couple of minutes; at this stage, two absorption bands at lower frequency appear (asterisks in Fig. 7a), associated with liquid-like ethylene condensed into the pores of the glass. This means that, due to the condensation effect, ethylene concentration in the pores is close to that of the liquid. Meanwhile, ethylene condenses inside the pores, two absorption bands start to grow at 2929 cm^{-1} and 2852 cm^{-1}, and are attributed to the asymmetric and symmetric ν(CH_2) vibrations of the growing polymeric chains. A detail of the first spectra in the region of the 2852 cm^{-1} absorption band is reported in the inset of Fig. 7a: despite the high dilution of the chromium centers, evidence of an "anomalous band" due to metallacycle intermediates is observed at 2863 cm^{-1}, demonstrating that the initiation mechanism is the same as that demonstrated to occur on Cr(II)/aerosil [56].

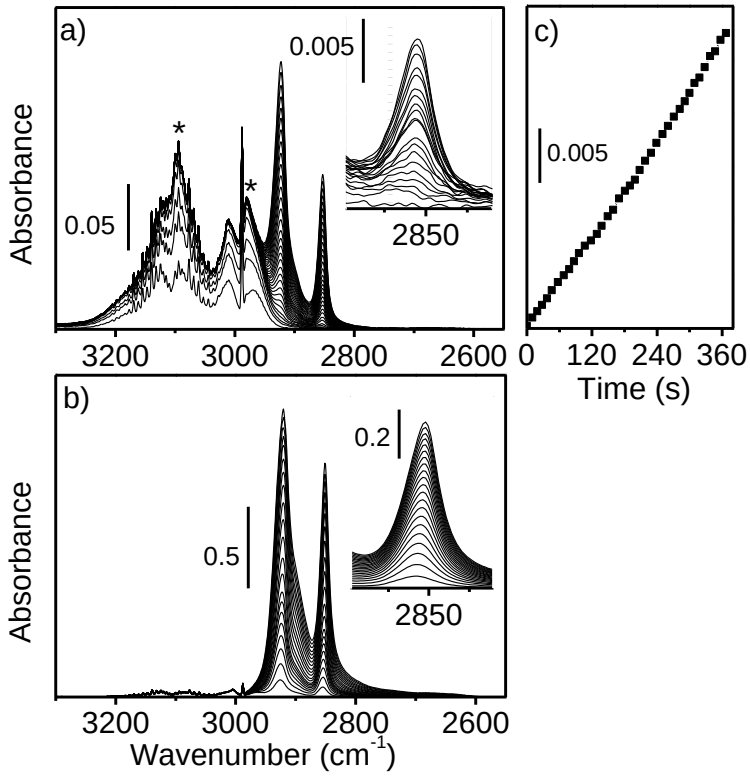

Fig. 7. Time-resolved FT-IR spectra collected during ethylene polymerization at room temperature on Cr0.01M (part a) and Cr1.0P (part b). In the inset of both parts, an enlargement of the respective absorption bands at 2852 cm^{-1} is given, where the first steps of polymerization are shown. Asterisks in part a) indicate the IR absorption bands due to liquid-like ethylene condensed in the monolith's pores. Part c) shows the intensity of IR band at 2853 cm^{-1} versus time during polymerization of ethylene on Cr0.01M.

A similar FT-IR experiment during ethylene polymerization was performed on Cr1.0P; the spectra in the ν(CH_2) region are reported in Fig. 7b. By comparing the two set of data, some important points can be addressed: (i) it is clear that in both cases no evidence of methyl or other termination groups are present in the FT-IR spectra; (ii) as the chromium concentration in Cr0.01M is two orders of magnitude smaller than in Cr1.0P, the similarity of the spectra of the obtained polyethylene strongly suggests that Cr0.01M system can be considered as a highly diluted model for Phillips catalyst.

Finally, the number of sites involved in ethylene polymerization was roughly estimated by comparing the FT-IR spectra of CO adsorbed on the sample before and after the polymerization [54] (here not shown). It was found that about 50% of sites are involved in the reaction in Cr0.01M; i.e. 5 times more than in standard Cr(II)/aerosil samples. No doubt, these findings have to be further confirmed by data coming from other techniques. As a tentative explanation we propose that the presence of liquid-like ethylene in the monolith pores (confirmed by bands marked by asterisks in Fig. 7, part a) favors initiation of polymer growth also on chromium sites which are usually spectators. As for the ethylene polymerization activity (calculated per Cr center) is concerned, the analysis of the data obtained on 0.01 and 0.1 samples (Fig. 7c) suggests that in this concentration interval the activity is independent upon the Cr content. This fact is a further proof that the participation of more than one chromium site in polymer growth is unlikely.

In a successive step, ethylene polymerization reaction on both Cr0.01M and Cr0.5P was monitored by UV–Vis spectroscopy both in transmission and DR modes. The results are compared in Fig. 8. When ethylene is dosed on Cr0.01M sample, the UV–Vis spectrum in the CT region is perturbed in a similar way to what observed in presence of CO (Fig. 6a): the CT band at 30,000 cm^{-1}, characteristic of highly coordinatively unsaturated Cr(II) species, decreases in intensity in favor of a new band at 36,000 cm^{-1} (bold gray curve), testifying the formation of the Cr(II)/ethylene adducts. Successively, a rapid modification of the scattering properties of the sample is observed, due to the growth of polymer chains that fill the monolith pores, with the consequent increase in the opacity of the glass. Therefore, it is not possible to extract information on the CT transitions characteristic of the Cr sites active in ethylene polymerization. The occurrence of a successful ethylene polymerization is testified by the appearance of well defined bands in the NIR region (see inset in Fig. 8a), due to overtone and combination modes of the polyethylene vibrations.

The results of a similar experiment performed in reflectance mode on Cr0.5P sample are shown in Fig. 8b. The evolution of the CT band at 30,000 cm^{-1} is very similar to that previously discussed for Cr0.01M. In the range of d–d transitions, the main effect of ethylene dosage is the disappearance of the d–d doublet at 12,000 and 7500 cm^{-1} characteristic of Cr(II) sites, in favor of a new component at 16,350 cm^{-1} which is ascribable to the formation of Cr(II)/ethylene adducts. To the best of our knowledge, this is the first report on the optical properties of Cr(II) sites in interaction with ethylene monomer. Upon waiting in time a progressive restoration of the original doublet is observed. This phenomenon suggests that ethylene is consumed from the “dormant sites” (i.e. ethylene pressure is reduced). The occurrence of an extensive ethylene

polymerization is testified also in this case by the appearance of the combination/overtone bands of the polymer (inset of Fig. 8b). Unfortunately, no additional bands assignable to the Cr sites involved in the polymerization are observed, preventing any discussion on the formal oxidation state of the Cr sites during the polymerization reaction. In this respect, further investigation is planned.

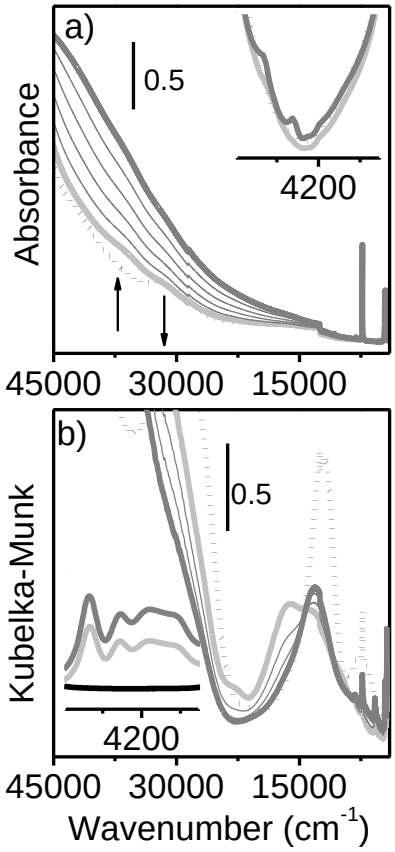

Fig. 8. UV-Vis spectra collected during ethylene polymerization at room temperature on Cr0.01M (recorded in transmittance, part a) and on Cr0.5P (acquired in reflectance mode, part b). Dotted spectra: Cr(II)/SiO_2 samples before ethylene dosage; bold light grey spectra: first spectra after ethylene dosage; bold grey spectra: last recorded after ethylene polymerization The intermediate steps are shown in grey. Both insets show the magnification of the region where the overtones and combination modes of polyethylene are observable.

At the end of polymerization experiment, the composite monolith was immersed in HF to dissolve the silica part. In this way a polymeric monolith was obtained and observed by SEM (Fig. 9). Parts (a) and (b) represent the external surface of the monolith "top view", while parts (c) and (d) show images obtained on a portion of the polymer cut vertically. Section (e) shows a macroscopic view of the piece of polymer which exactly reproduces the original shape of the silica monolith. The images clearly show the fibrous nature of the polymer that was formed inside the mesopores of the monolith. The regularity of the samples both from top and side views indicates that the polymerization was homogeneously occurred inside the whole monolith.

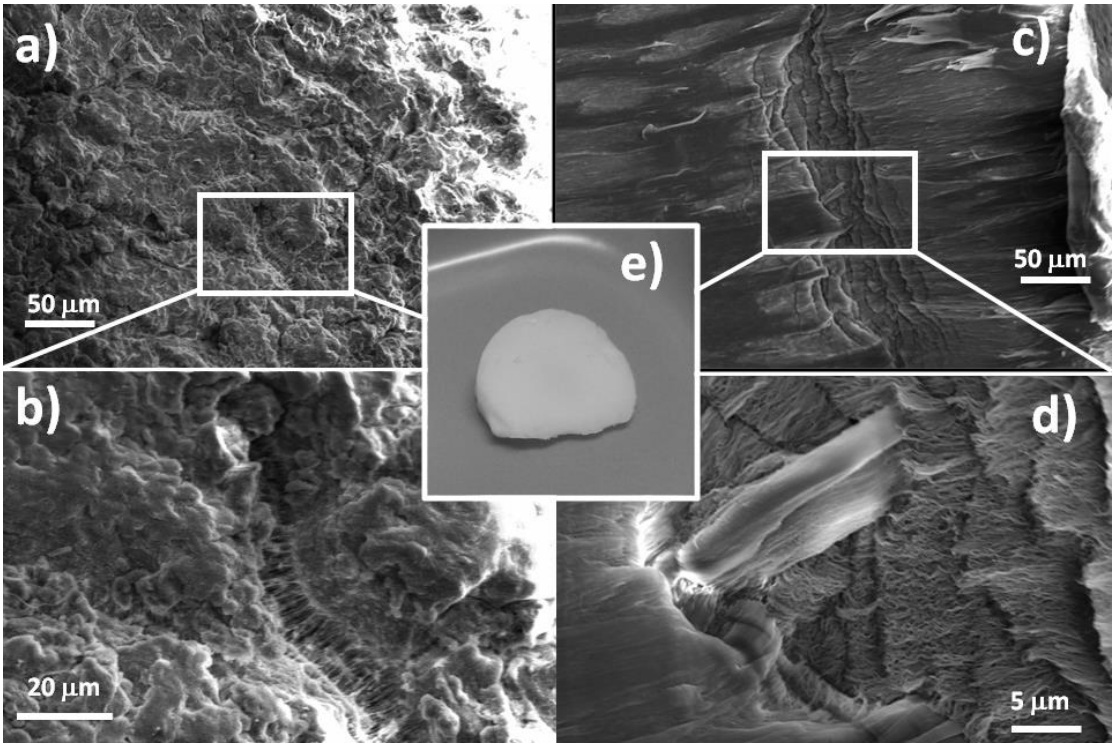

Fig. 9. SEM images of a polymer portion grown on the Cr-doped monolith. Top view is reported in part a) with a detail enlarged in part b); lateral section is presented in part c) with a detail enlarged in part d). The picture of the whole polymer formed is shown in part e).

4. Conclusions

Pure and Cr-doped silica mesoporous monoliths with very high surface area have been synthesized by one-pot sol–gel method. It is demonstrated that Cr-doped monoliths can be adopted as models for spectroscopic studies of very diluted Phillips catalyst. Indeed, the possibility to obtain slices of suitable thickness without appreciable scattering in the whole IR and UV–Vis–NIR region allows to increase the sensitivity and to fully characterize very diluted samples by means of standard transmission spectroscopies. In particular, it was possible to collect UV–Vis–NIR spectra in transmittance of both oxidized and reduced samples, obtaining unprecedented information on the relative intensity of bands due to charge transfer and d–d transitions, not possible by diffuse reflectance spectroscopy. Moreover, FT-IR spectroscopy of adsorbed CO (used as a probe of the Cr structure) revealed that, also when Cr is extremely diluted (Cr0.01M sample), a distribution of chromium species differing in their coordination ability is present, very similar to that found on 100 times more concentrated aerosil-based samples (Cr1.0P). Therefore, the structural heterogeneity of chromium sites characteristic of Phillips catalyst (and likely responsible of the broad molecular weight distribution of the polyethylene product) is not related neither to the chromium concentration nor to the properties of the silica support, but seems to be an intrinsic property of the Cr/SiO_2 system.

The grafted Cr(II) species readily react at room temperature with ethylene gas with the consequent fast growth of high density polyethylene. Ethylene condenses into the glass

pores even at relatively low pressure; as a consequence, the number of sites involved in ethylene polymerization was roughly estimated to be 5 times higher than on standard, aerosil-based, Phillips catalyst. Moreover, the similarity of the in situ FT-IR spectra of the growing polymer and the substantially unvarying reaction rate calculated per Cr center for the two cases strongly suggests that the participation of more than one chromium site in polymer growth in the standard Phillips catalyst is unlikely. This study complements previous works from our group where a model of the Phillips catalyst was obtained after impregnation with CrO_3 a silica aerogel; the obtained material behaved as an optically uniform medium in the spectral region used to perform UV–Vis, IR and Raman experiments [58] and [59].

Finally, the Cr-doped silica monoliths offered the opportunity to obtain highly porous, silica-free, polyethylene monoliths, as replicas of the catalyst structure (after dissolution of the silica in HF).

5. Acknowledgements

We thank Dott. Ivana Miletto for SEM micrographs. Financial support was provided by "Progetti di Ricerca di Ateneo-Compagnia di San Paolo-2011- Linea 1A" (ORTO11RRT5 project).

References

[1] M.P. McDaniel, Adv. Catal. 53 (2010) 123–606.

[2] J.P. Hogan, R.L. Banks, Polymers and Production thereof U.S.P. Office, United States, 1958.

[3] M.P. McDaniel, Adv. Catal. 33 (1985) 47–98.

[4] B.M. Weckhuysen, I.E. Wachs, R.A. Schoonheydt, Chem. Rev. 96 (1996) 3327–3349.

[5] B.M. Weckhuysen, R.A. Schoonheydt, Catal. Today 51 (1999) 215–221.

[6] E. Groppo, C. Lamberti, S. Bordiga, G. Spoto, A. Zecchina, Chem. Rev. 105 (2005) 115–183.

[7] E. Groppo, K. Seenivasan, C. Barzan, Catal. Sci. Technol. 3 (2013) 858–878.

[8] I.E. Wachs, C.A. Roberts, Chem. Soc. Rev. 39 (2010) 5002–5017.

[9] G. Ghiotti, E. Garrone, A. Zecchina, J. Mol. Catal. 46 (1988) 61–77.

[10] D. Gianolio, E. Groppo, J.G. Vitillo, A. Damin, S. Bordiga, A. Zecchina, C. Lamberti, Chem. Commun. 46 (2010) 976–978.

[11] B.P. Liu, M. Terano, J. Mol. Catal. A 172 (2001) 227–240.

[12] K. Tonosaki, T. Taniike, M. Terano, J. Mol. Catal. A – Chem. 340 (2011) 33–38.

[13] D.S. McGuinness, N.W. Davies, J. Horne, I. Ivanov, Organometallics 29 (2010) 6111–6116.

[14] C. Moisii, E.W. Deguns, A. Lita, S.D. Callahan, L.J. van de Burgt, D. Magana, A.E. Stiegman, Chem. Mater. 18 (2006) 3965–3975.

[15] P.C. Thune, C.P.J. Verhagen, M.J.G. van den Boer, J.W. Niemantsverdriet, J. Phys. Chem. B 101 (1997) 8559–8563.

[16] P.C. Thune, J. Loos, D. Wouters, P.J. Lemstra, J.W. Niemantsverdriet, Macromol. Symp. 173 (2001) 37–52.

[17] E.M.E. van Kimmenade, A.E.T. Kuiper, Y. Tamminga, P.C. Thune, J.W. Niemantsverdriet, J. Catal. 223 (2004) 134–141.

[18] C.A. Demmelmaier, R.E. White, J.A. van Bokhoven, S.L. Scott, J. Catal. 262 (2009) 44–56.

[19] O. Espelid, K.J. Borve, J. Catal. 195 (2000) 125–139.

[20] O. Espelid, Theoretical Models of Active Sites at Cr/Silica Phillips-type Catalysts for Ethylene Polymerization. PhD Thesis in Chemistry, Bergen, Norway.
[21] A. Damin, J.G. Vitillo, G. Ricchiardi, S. Bordiga, C. Lamberti, E. Groppo, A. Zecchina, J. Phys. Chem. A 113 (2009) 14261–14269.
[22] H. Guesmi, F. Tielens, J. Phys. Chem. C 116 (2012) 994–1001.
[23] L. Zhong, Z. Liu, R. Cheng, S. Tang, P. Qiu, X. He, M. Terano, B. Liu, ChemCatChem 4 (2012) 872–881.
[24] J.P. Hogan, Applied Industrial Catalysis, Academic Press, New York, pp. 149–176.
[25] A. Zecchina, E. Garrone, G. Ghiotti, S. Coluccia, J. Phys. Chem. 79 (1975) 972–978.
[26] A. Zecchina, E. Garrone, G. Ghiotti, C. Morterra, E. Borello, J. Phys. Chem. 79 (1975) 966–972.
[27] A. Zecchina, E. Garrone, C. Morterra, S. Coluccia, J. Phys. Chem. 79 (1975) 978–983.
[28] C. Lamberti, E. Groppo, G. Spoto, S. Bordiga, A. Zecchina, Adv. Catal. 51 (2007) 1–74.
[29] C. Lamberti, A. Zecchina, E. Groppo, S. Bordiga, Chem. Soc. Rev. 39 (2010) 4951–5001.
[30] G. Ghiotti, E. Garrone, A. Zecchina, J. Mol. Catal. 65 (1991) 73–83.
[31] E. Garrone, S. Abello, E. Borello, G. Ghiotti, A. Zecchina, Mater. Chem. Phys. 29 (1991) 369–378.
[32] A. Zecchina, C.O. Arean, E. Groppo, ChemCatChem 2 (2010) 259–262.
[33] A.E. Stiegman, J. Eckert, G. Plett, S.S. Kim, M. Anderson, A. Yavrouian, Chem. Mater. 11 (1993) 1591–1594.
[34] M.D. Curran, T.E. Gedris, A.E. Stiegman, G. Plett, Chem. Mater. 11 (1999) 1120–1127.
[35] C. Weiping, Z. Lide, J. Phys.: Condens. Matter 9 (1997) 7257–7267.
[36] S. Brunauer, P.H. Emmett, E. Teller, J. Am. Chem. Soc. 60 (1938) 309–319.
[37] E.P. Barrett, L.G. Joyner, P.P. Healenda, J. Am. Chem. Soc. 73 (1951) 373–380.
[38] B. Witschas, in: U. Schumann (Ed.), Atmospheric Physics, Springer-Verlag, Berlin Heidelberg, pp. 69–83.
[39] K.S.W. Sing, D.H. Everett, R.A.W. Haul, L. Moscou, R.A. Pierotti, J. Rouquerol, T. Siemiemewska, Pure Appl. Chem. 57 (1985).
[40] J. Rouquerol, D. Avnir, C.W. Fairbridge, D.H. Everett, J.M. Haynes, N. Pernicone, J.D.F. Ramsay, K.S.W. Sing, K.K. Unger, Pure Appl. Chem. 66 (1994).
[41] F.J.R. Rouquerol, K. Sing, Adsorption by Powders and Porous Solids: Principles, Methodology and Applications, Academic Press, London, 1999.
[42] L.T. Zhuravlev, Colloids Surf. A 173 (2000) 1–38.
[43] G.D. Chukin, A.I. Apretova, J. Appl. Spectrosc. 50 (1989) 418–422.
[44] C.C. Perry, X. Li, J. Chem. Soc. Faraday Trans. 87 (1991) 761–766.
[45] C.C. Perry, X. Li, J. Chem. Soc. Faraday Trans. 87 (1991) 3857–3862.
[46] A. Burneau, C. Carteret, Phys. Chem. Chem. Phys. 2 (2000) 3217–3226.
[47] B.N. Figgis, Introduction to Ligand Fields, John Wiley & Sons, New York, 1966.
[48] B.M. Weckhuysen, L.M. Deridder, R.A. Schoonheydt, J. Phys. Chem. 97 (1993) 4756–4763.
[49] B.M. Weckhuysen, R.A. Schoonheydt, J.M. Jehng, I.E. Wachs, S.J. Cho, R. Ryoo, S. Kijlstra, E. Poels, J. Chem. Soc. Faraday Trans. 91 (1995) 3245–3253.
[50] A. Zecchina, G. Spoto, G. Ghiotti, E. Garrone, J. Mol. Catal. 86 (1994) 423–446.
[51] B. Rebenstorf, R. Larsson, Z. Anorg, Allg. Chem. 478 (1981) 119–138.
[52] L. Zhong, M.Y. Lee, Z. Liu, Y.J. Wanglee, B.P. Liu, S.L. Scott, J. Catal. 293 (2012) 1–12.
[53] M.P. McDaniel, S.J. Martin, J. Phys. Chem. 95 (1991) 3289–3293.
[54] E. Groppo, C. Lamberti, F. Cesano, A. Zecchina, Phys. Chem. Chem. Phys. 8 (2006) 2453–2456.

[55] E. Groppo, C. Lamberti, G. Spoto, S. Bordiga, G. Magnacca, A. Zecchina, J. Catal. 236 (2005) 233–244.
[56] E. Groppo, C. Lamberti, S. Bordiga, G. Spoto, A. Zecchina, J. Catal. 240 (2006) 172–181.
[57] B. Liu, H. Nakatani, M. Terano, J. Mol. Catal. A 184 (2002) 387–398.
[58] E. Groppo, A. Damin, F. Bonino, A. Zecchina, S. Bordiga, C. Lamberti, Chem. Mater. 17 (2005) 2019–2027.
[59] A. Damin, F. Bonino, S. Bordiga, E. Groppo, C. Lamberti, A. Zecchina, ChemPhysChem 7 (2006) 342–344